Scaling Theory for the Frictionless Unjamming Transition

Kabir Ramola

Martin Fisher School of Physics,
Brandeis University

In collaboration with Bulbul Chakraborty

July 22, 2016

Introduction

- The **unjamming transition** of soft spheres exhibits properties **reminiscent of critical points** in equilibrium systems, with observed power laws and scaling collapses of dynamical quantities.
- How does one build a **microscopic theory using packing fraction**?
- We develop a statistical framework for the transition using **local grain areas assigned to each contact** that play the role of "quasiparticles".
- We use the **underlying distributions of interparticle distances and angles** to derive a density of states of these areas.
- We find that the scaling with energy near the transition can be attributed to **divergences in the density of states**.
- We show that in order to understand the scaling behaviour near the transition, one needs to account for **three-body interactions**.

Jammed Packings

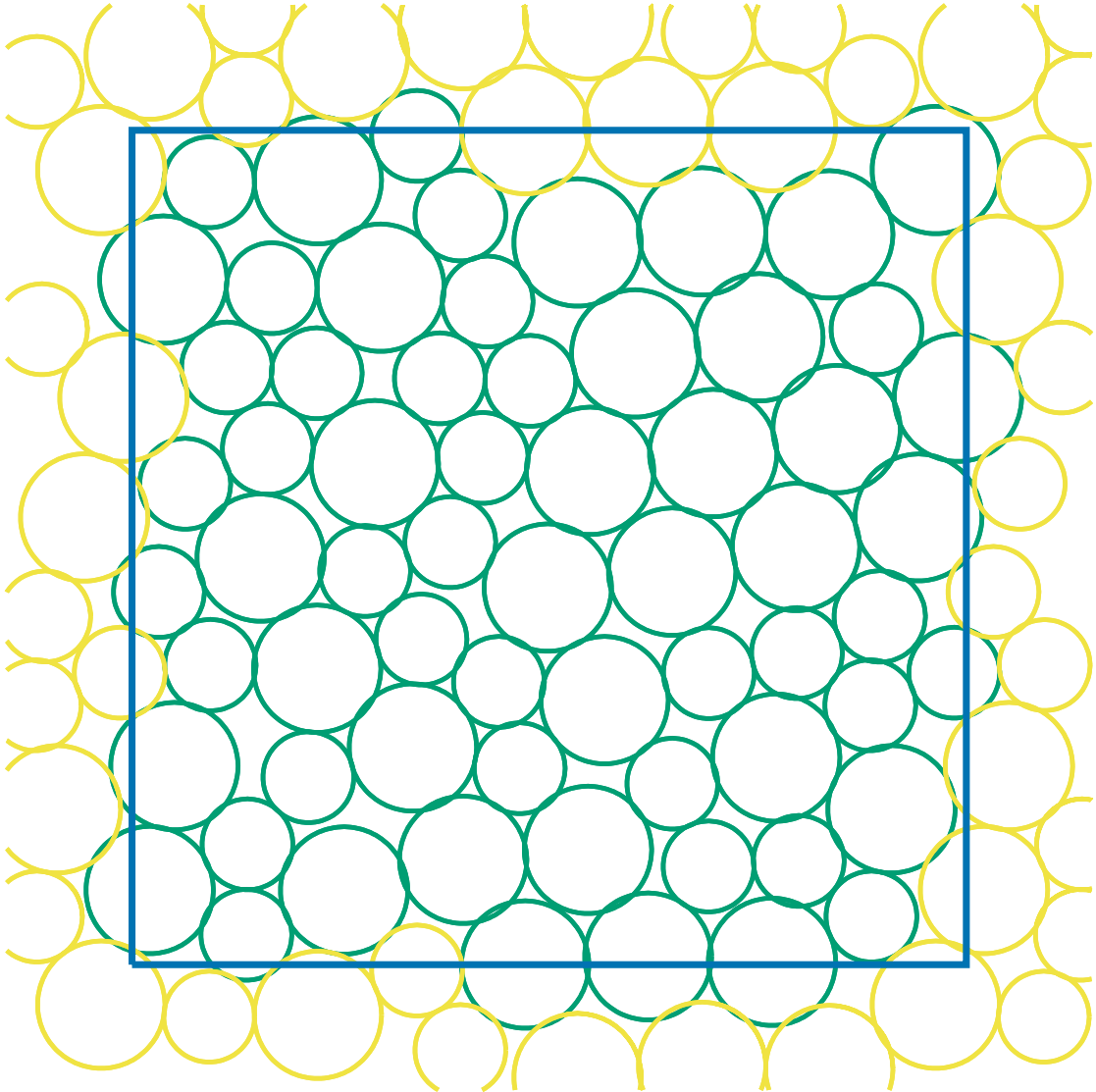

Jammed Packings: Contact Points

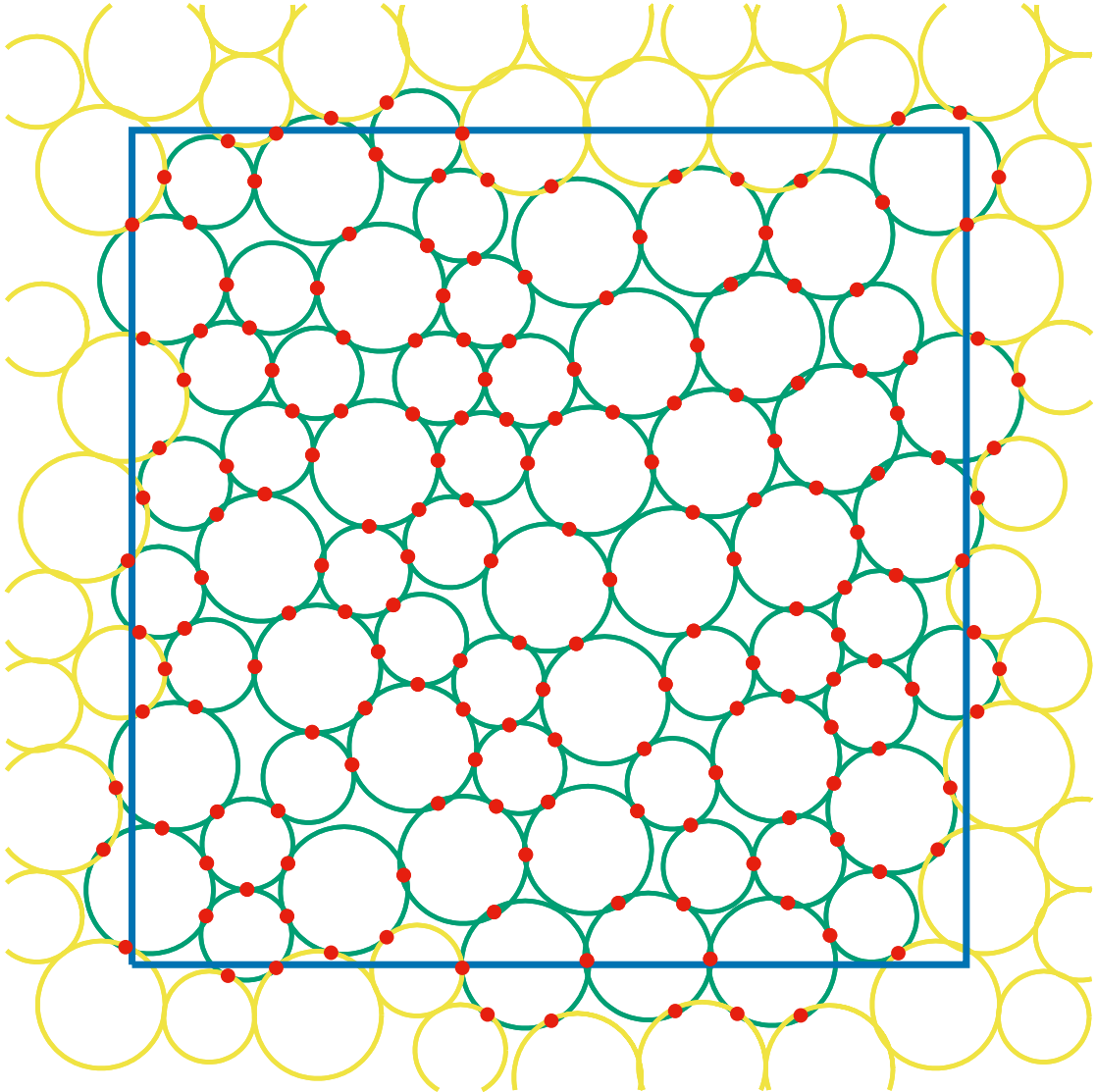

Jammed Packings: Minimum Cycle Basis

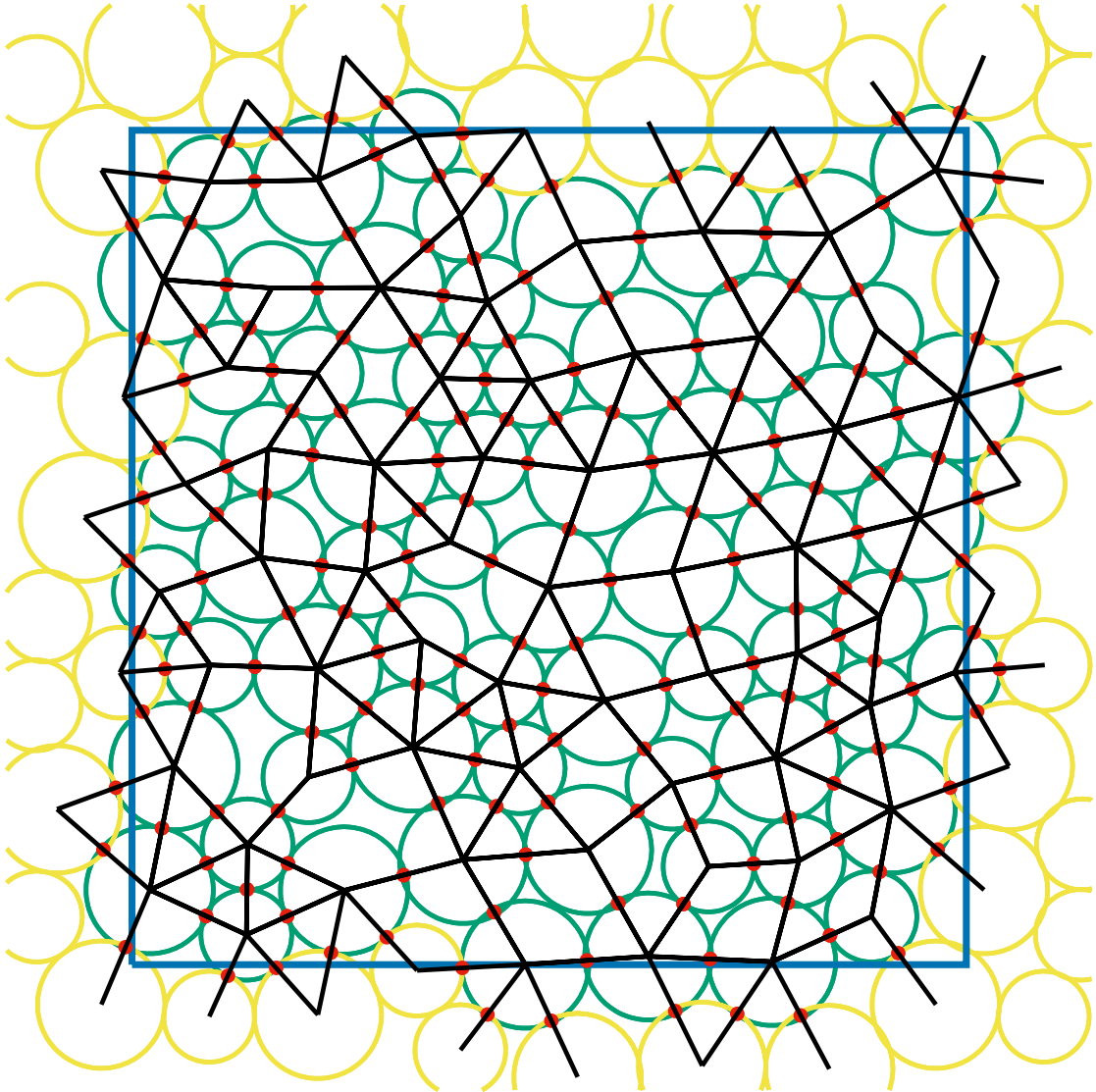

Partition Function

- The partition function at a fixed energy E_G is given by

$$\Omega(E_G) = \int \mathcal{D}[\{\vec{r}_g, \sigma_g\}] \delta\left(E_G - V[\{\vec{r}_g, \sigma_g\}]\right) \delta\left(\frac{\partial V[\{\vec{r}_g, \sigma_g\}]}{\partial \vec{r}_g}\right). \tag{1}$$

- Jammed states are characterised by a **system spanning contact network**.
- For **frictionless disks** this naturally partitions the space into **convex minimum cycles** (or faces) of z_v sides each.
- The **loop constraints** around each face can be implemented as

$$\{\vec{r}_g\} \to \{\vec{r}_{g,g'}\} \times \prod_v \delta\left(\sum_{i=1}^{z_v} \vec{r}^{\,i}_{g,g'}\right), \quad \text{with} \quad \vec{r}_{g,g'} = \vec{r}_{g'} - \vec{r}_g. \tag{2}$$

Jammed Packings: Grain Polygons and Void Polygons

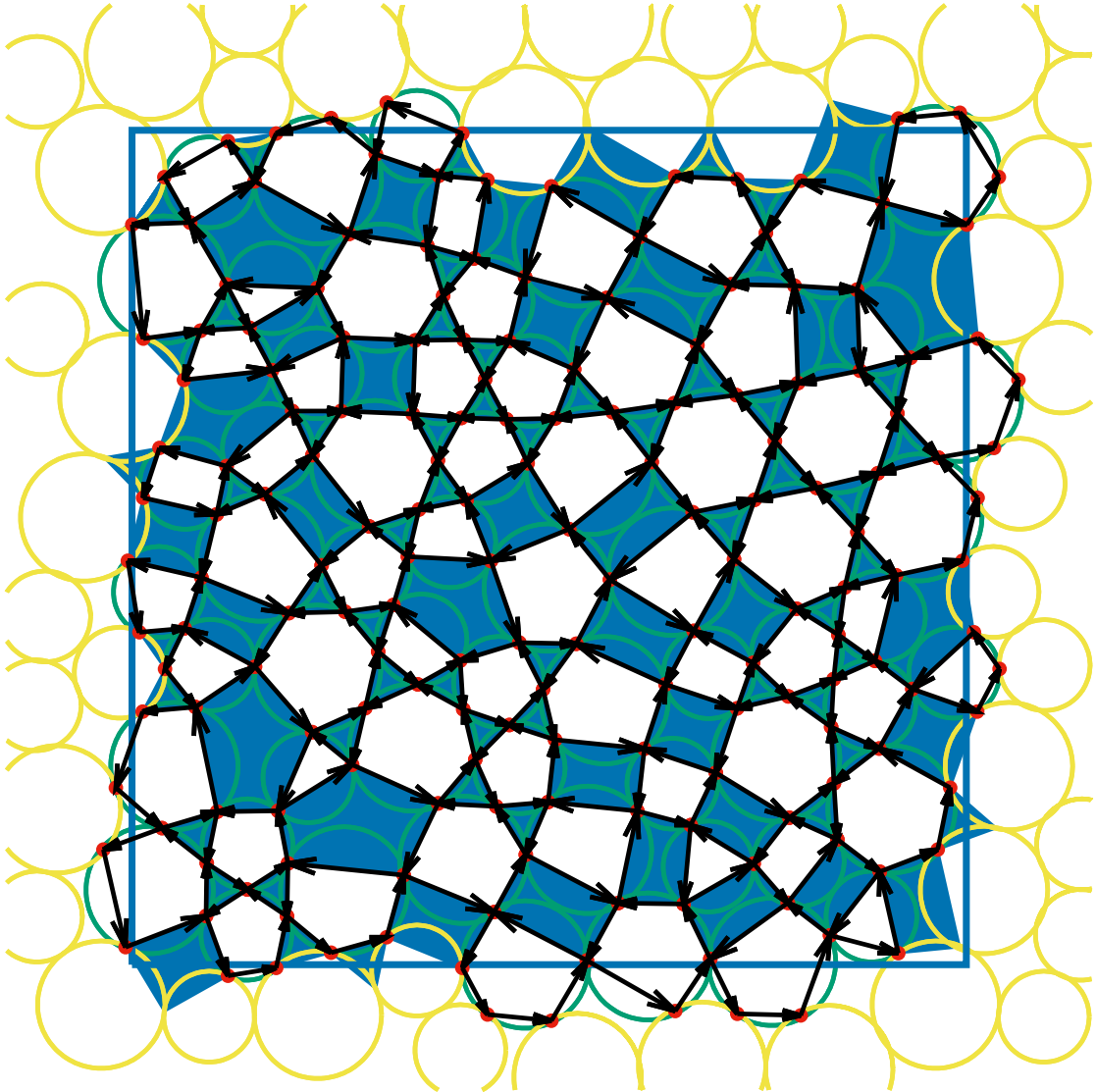

Edge Triangles and Local Areas

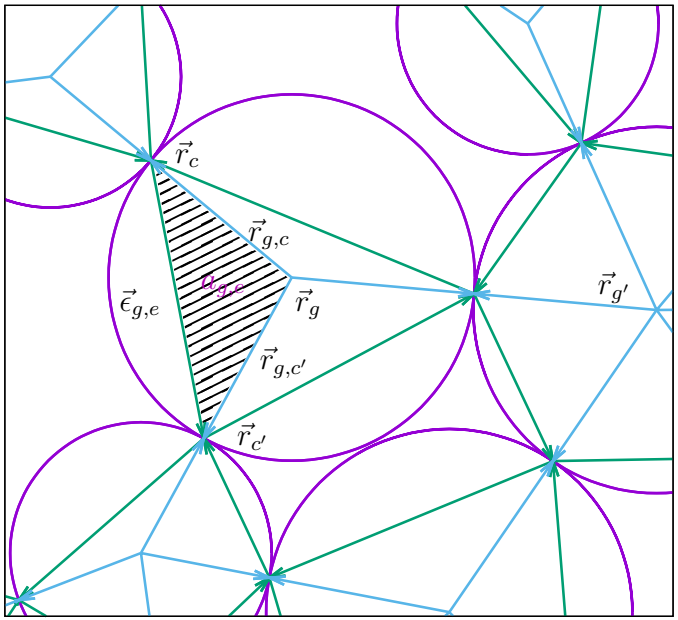

Figure: A section of a jammed configuration. The shaded area is referred to as an **edge triangle** and can be assigned uniquely to each contact.

- These basic triangular units are the **local measure of density (packing fraction)** in our description:

$$\alpha_e = \frac{a_{g,e}}{\sigma_g^2} \quad \in \quad \left[0, \frac{1}{2}\right]. \tag{3}$$

Partition Function and Local Distributions

- We can express the partition function in terms of the joint density of states of these local areas

$$\Omega(E_G, N_C) = \left(\prod_{i=1}^{N_C} \int_0^{1/2} d\alpha_i \right) g_{E_G} \left(\alpha_1, \alpha_2, ..., \alpha_{N_C} \right). \tag{4}$$

- Similarly we can compute probability distributions

$$p_{E_G}(\alpha_1) = \left(\prod_{i=2}^{N_C} \int_0^{1/2} d\alpha_i \right) \frac{g_{E_G} \left(\alpha_1, \alpha_2, ..., \alpha_{N_C} \right)}{\Omega(E_G, N_C)}. \tag{5}$$

- In real systems (and simulations), the number of contacts N_C **is a fluctuating quantity**.

Numerical Simulations

- Configurations are produced using the O'Hern protocol.
- The interaction potential between the particles is modeled as a **soft linear spring repulsion** potential of the form:

$$V(\{\vec{r}_g, \sigma_g\}) = \sum_{g \neq g'} \frac{1}{2} \left(1 - \frac{|\vec{r}_{g,g'}|}{\sigma_{g,g'}}\right)^2 \Theta\left(1 - \frac{|\vec{r}_{g,g'}|}{\sigma_{g,g'}}\right), \qquad (6)$$

  where Θ is the Heaviside function, $\vec{r}_{g,g'} = \vec{r}_g - \vec{r}_{g'}$ and $\sigma_{g,g'} = \sigma_g + \sigma_{g'}$.
- We simulate **bidispersed** configurations with diameter ratio $(1 : 1.4)$.
- We use **periodic boundary conditions** in both directions, the configurations are in a box size 1 (i.e. $L_x = L_y = 1$).

Total Grain Area

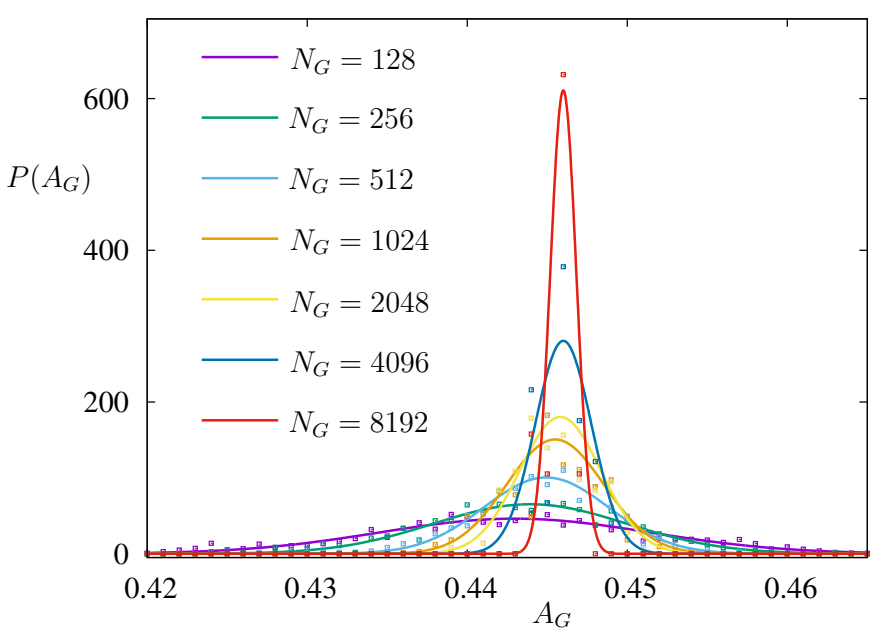

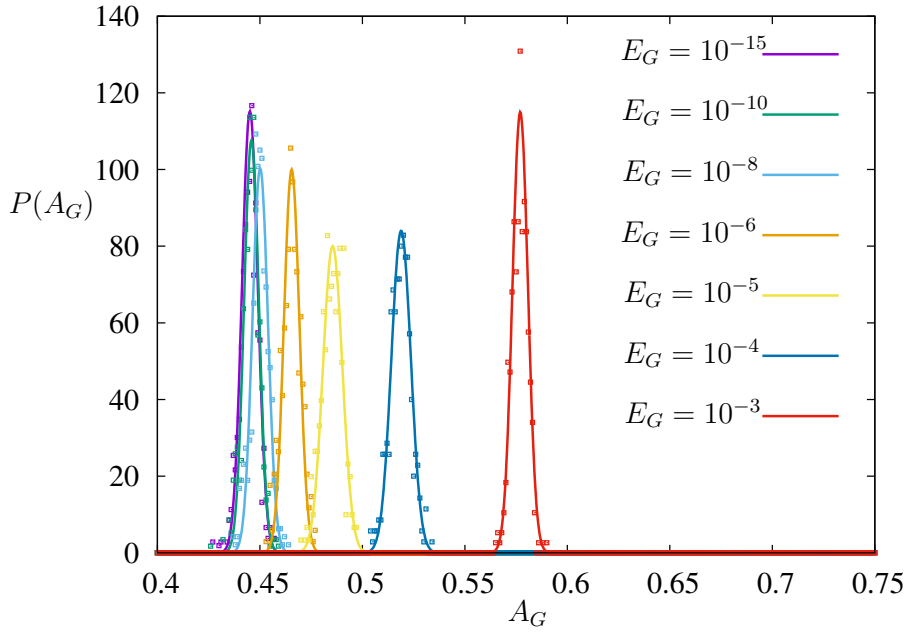

Figure: **(Left)** Distribution of the total area covered by the grain polygons A_G at $E_G = 10^{-15}$. Using finite-size scaling fits we find is $A_G^* = 0.446(1)$ as the number of grains $N_G \to \infty$ and $E_G \to 0^+$. **(Right)** Behaviour of the grain area distributions for different energies for packings of $N_G = 512$ disks.

Scaling with Energy

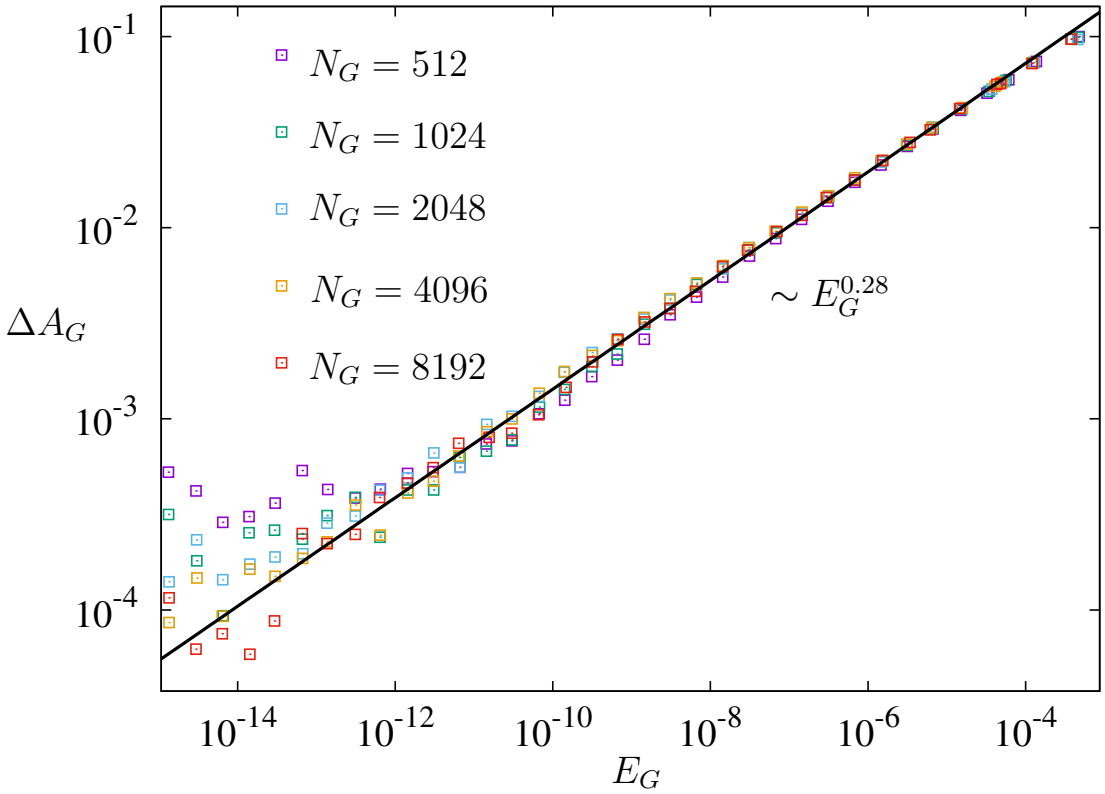

Figure: Scaling of the excess grain area $\Delta A_G = A_G - A_G^*$ with total energy per particle E_G. We find that the excess grain area scales as a power of the total energy in the system with exponent $\beta_E = 0.28(2)$.

Scaling with Coordination

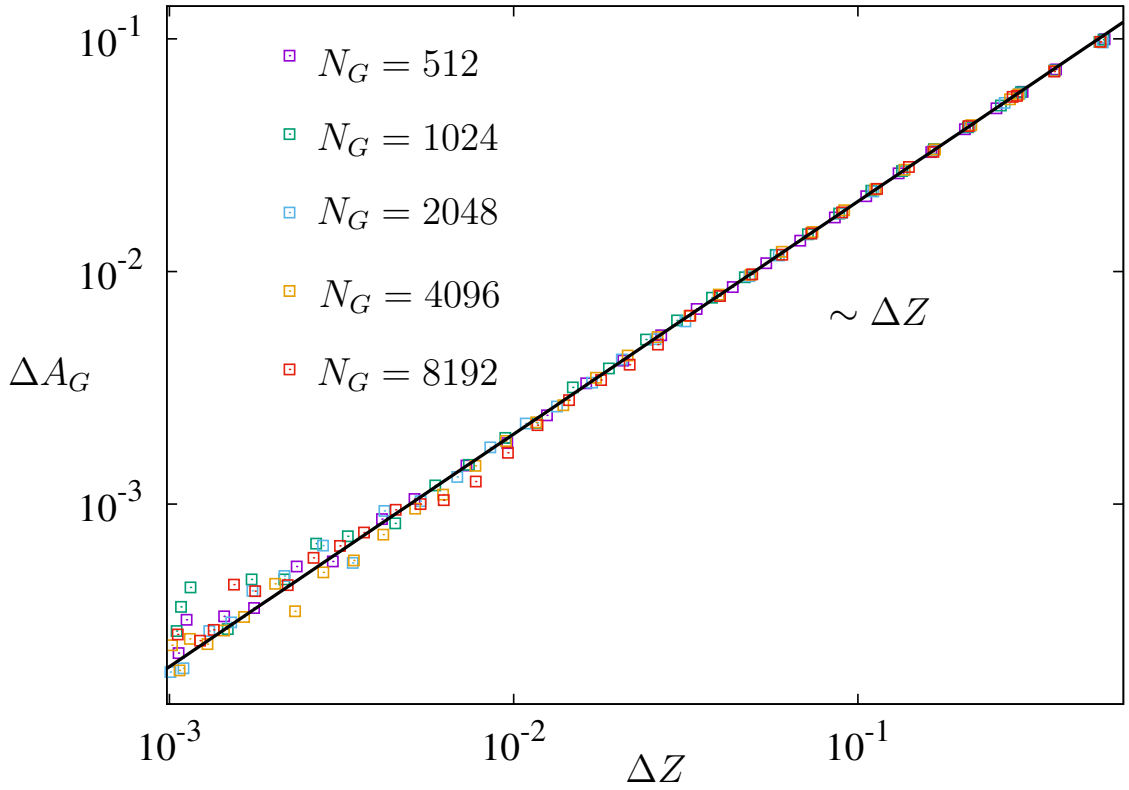

Figure: Scaling of ΔA_G with excess coordination in the system ΔZ. We find that the excess grain area scales as a power of ΔZ with exponent $\beta_Z = 1.00(1)$.

Local Area Distribution

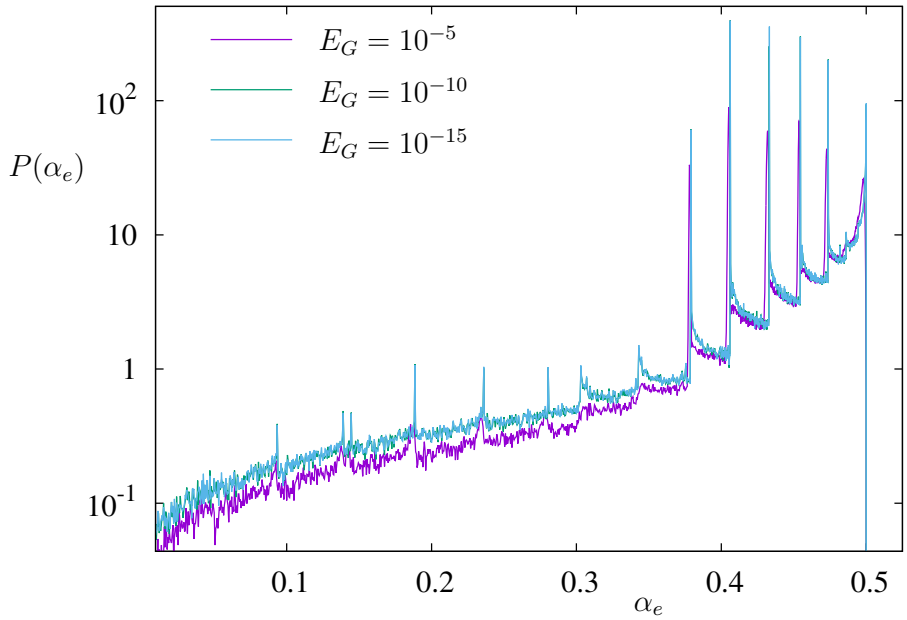

Figure: Distribution of areas of the edge triangles $\alpha_e = a_{g,e}/\sigma_g^2$ for $N_G = 2048$. $\alpha_e \to 1/2$ corresponds to disks with relative contact angles close to $\pi/2$. We find well defined ordered peaks that can be used to estimate the amount of order in the system. The five largest peaks arise from three-disk crystallization. These ordered peaks get sharper as $E_G \to 0^+$.

Scaling Collapse

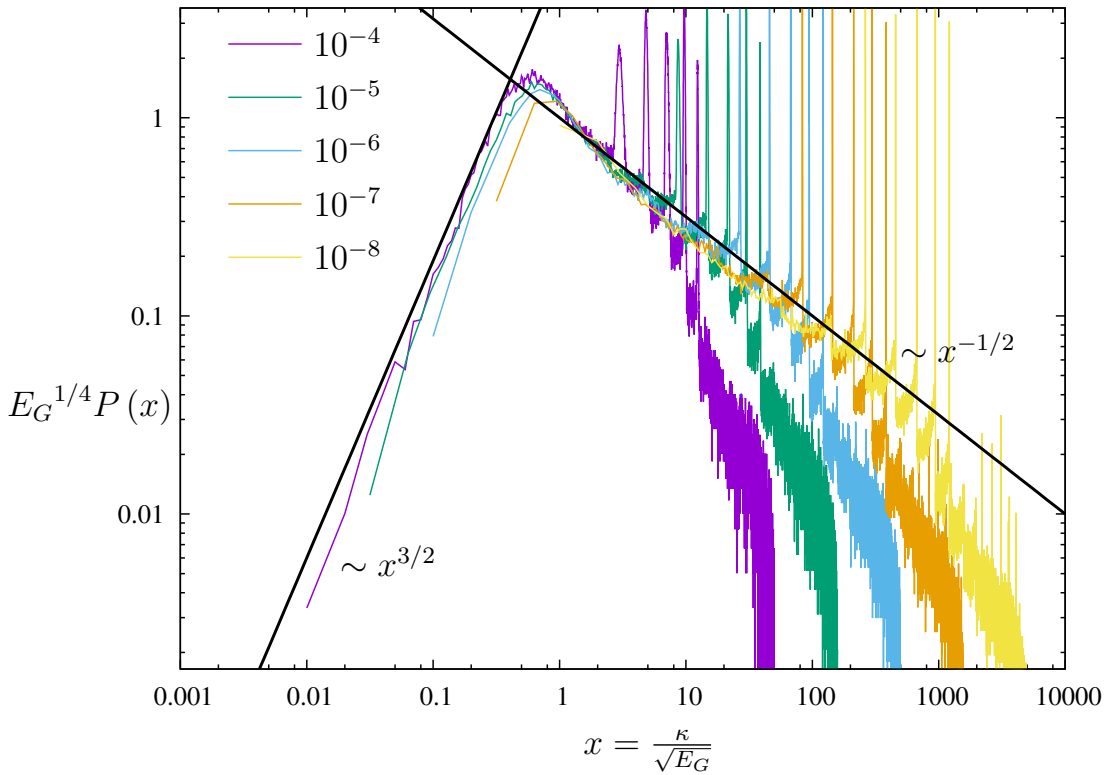

Figure: Scaling collapse of the distribution of areas of the edge triangles. The plot shows the distribution of $\kappa = \left(\frac{1}{2} - \frac{a_{g,e}}{{\sigma_g}^2}\right)$ for $N_G = 512$.

Ordered Structures

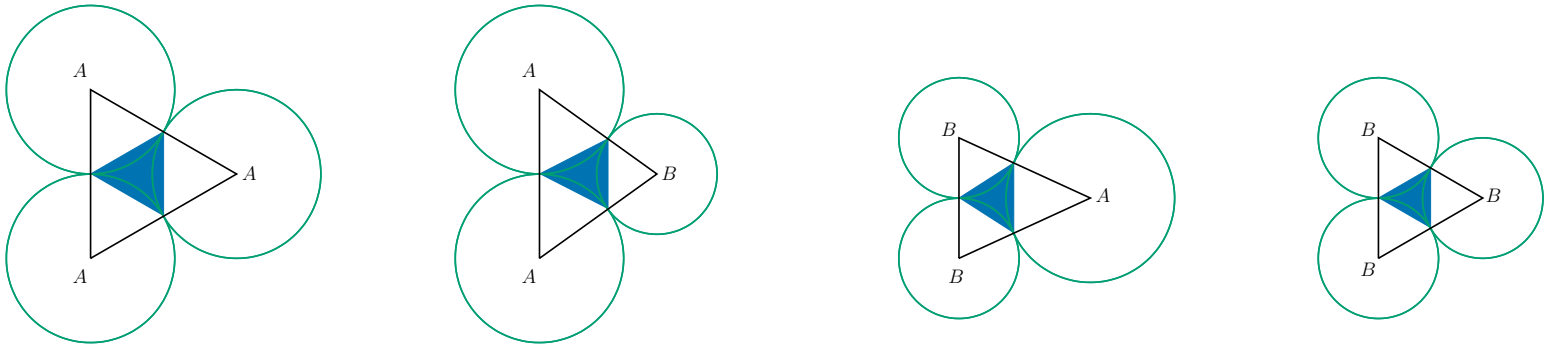

Figure: The four three-disk crystallization configurations that can occur in bidispersed systems. This causes ordered peaks to appear in the distribution of edge triangle areas (white triangles) and the areas of void polygons (blue triangles). The fraction of the system in these ordered structures gives us a measure of order in the system.

- We **focus on the** $A - A - A$ **case**. The generalization to the polydisperse case is straightforward.

Building a Theory

- We **assume a product form** for the joint distribution of areas

$$p(a_1, a_2, ...a_{N_C}) = \prod_{i=1}^{N_C} p(a). \tag{7}$$

- The distribution of individual areas is given by

$$p(a) = \int d\vec{r}_1 \int d\vec{r}_2 \; p(\vec{r}_1, \vec{r}_2) \; \delta \left(\frac{|\vec{r}_1 \times \vec{r}_2|}{2} - a \right). \tag{8}$$

  where $\vec{r}_1$ and $\vec{r}_2$ are the contact vectors bounding the triangle.
- The one point distribution is **independent of orientation**

$$p(\vec{r}_1) = \int d^2\vec{r}_2 p(\vec{r}_1, \vec{r}_2) = \frac{1}{2\pi} p(|\vec{r}_1|). \tag{9}$$

- The **joint distribution** can be decomposed as

$$p(\vec{r}_1, \vec{r}_2) = p(|\vec{r}_1|)p(|\vec{r}_2|)p(\sin\theta). \tag{10}$$

Local Areas

- In terms of the **scaled distances** $\vec{r} \to \vec{r}/\sigma_g$ we have

$$P(\alpha) = \int_0^1 dr_1 \int_0^1 dr_2 \int_0^1 d\sin\theta \; P(r_1)P(r_2)P(\sin\theta) \; \delta\left(\frac{1}{2} r_1 r_2 \sin\theta - \alpha\right). \tag{11}$$

- $\alpha < 1/2$ combined with the delta function produces a singularity in $p(\alpha)$ as $r_1 \to 1$, $r_2 \to 1$ and $\theta \to \pi/2$.

- Therefore **the relative angle between contact vectors is crucial** in determining the nature of the divergence as $E_G \to 0^+$.

Underlying Distributions: Contact Vector Lengths

- Contact lengths are **fluctuating quantities**

$$|\vec{r}| = \sigma_g - \Delta r \quad \text{with} \quad 0 < \Delta r < \sigma_g \tag{12}$$

- For linear spring potentials

$$E_G = \frac{1}{N_G} \sum_{i=1}^{N_C} (\Delta r_i)^2 \tag{13}$$

- We assume the contact fluctuations are drawn from a **uniform distribution with an energy dependent width** $\sqrt{E_G}$

$$p\left(r = \frac{|\vec{r}|}{\sigma_g}\right) = \frac{1}{\sqrt{E_G}} \Theta\left(r - 1 + \sqrt{E_G}\right) \Theta\left(1 - r\right) \tag{14}$$

- This is **independent of the cycle** to which it belongs

Observed Underlying Distributions

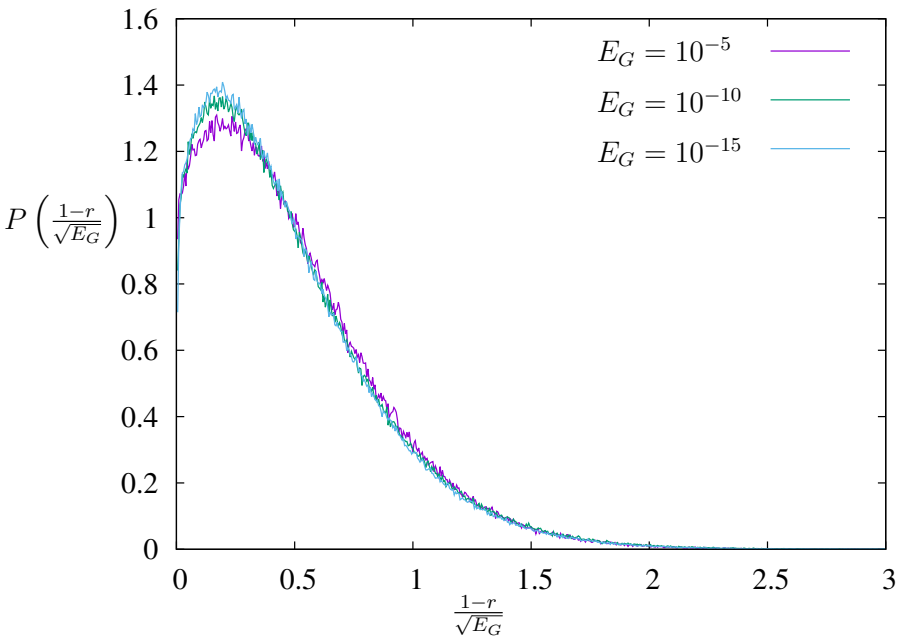

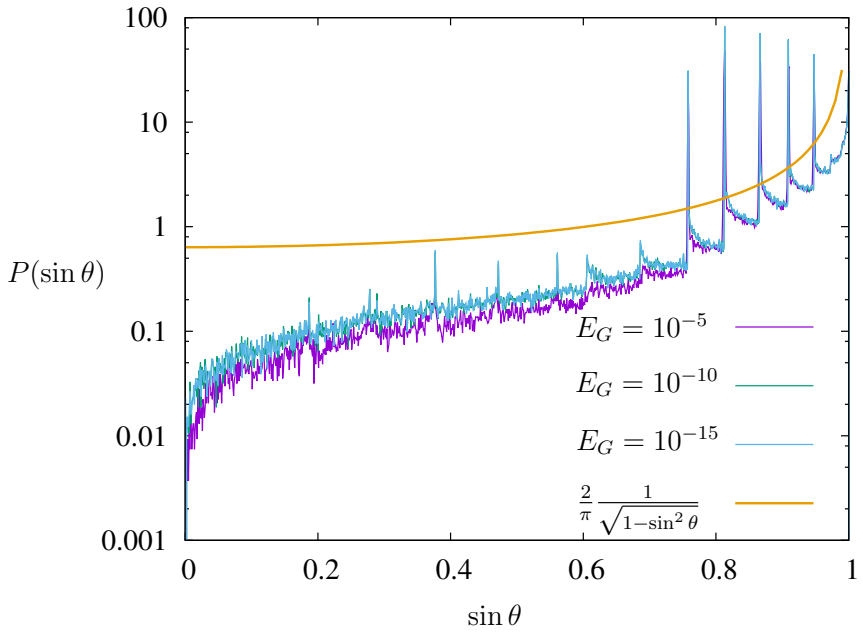

Figure: **(Left)** Distribution of lengths of contact vectors measured in packings with $N_G = 2048$ at different energies. The plot shows the distribution of $(1-r)/\sqrt{E_G}$, where $r = |\vec{r}_{g,c}|/\sigma_g$. **(Right)** Distribution of relative contact angles $\theta = \theta_{g,c'} - \theta_{g,c}$. These relative contact angles display random behaviour except at well-defined points that corresponds to crystallization angles. The five most prominent peaks can be identified as arising from three-disk crystallization.

Angular Distributions: > 3-minimum Cycles

- For $z_v > 3$ we have a **finite expansion about** $\theta = \pi/2$

$$p(\theta, > 3) = \frac{2}{\Delta} p(\pi/2) \quad \text{for} \quad \left|\theta - \frac{\pi}{2}\right| < \Delta \tag{15}$$

- Changing variables $\theta \to \sin\theta$

$$p(\sin\theta, > 3) = \frac{2p(\pi/2)}{\Delta\sqrt{1 - \sin^2\theta}} \quad \text{for} \quad \left|\theta - \frac{\pi}{2}\right| < \Delta \tag{16}$$

- We refer to the divergence in the area distribution arising from $\theta \to \pi/2$ as *disordered divergences*.

Angular Distributions: 3-minimum Cycles

- For $z_v = 3$ we have a distribution **centered at a finite value**

$$p(\theta, 3) \sim \frac{1}{\sqrt{E_G}} \mathcal{P}\left(\frac{\theta - \arcsin \frac{\sqrt{3}}{4}}{\sqrt{E_G}} \right). \tag{17}$$

- Changing variables $\theta \to \sin\theta$

$$p(\sin\theta, 3) \sim \frac{1}{\sqrt{1 - \sin^2\theta}} \frac{1}{\sqrt{E_G}} \tilde{\mathcal{P}}\left(\frac{\sin\theta - \frac{\sqrt{3}}{4}}{\sqrt{E_G}} \right). \tag{18}$$

- The contribution at $\theta = \pi/2$ is **exponentially suppressed**.
- This leads to an **integrable singularity** for the probability of areas.
- We refer to these as *ordered divergences*.

Ordered and Disordered Distributions

- We can **split the distribution into two classes** as follows

$$p(\alpha) = \frac{g(\alpha)}{N_C} = p(\alpha, 3) + \underbrace{p(\alpha, > 3)}_{p_{DO}(\alpha)+p_{\mathrm{reg}}(\alpha)} , \tag{19}$$

- with

$$p(3) = \int_0^{1/2} p(\alpha, 3) d\alpha, \qquad n(3) = N_C p(3), \tag{20}$$

- and

$$p(> 3) = \int_0^{1/2} p(\alpha, > 3) d\alpha, \qquad n(> 3) = N_C p(> 3). \tag{21}$$

Disordered Divergence: Exact Expression

- We can derive an **explicit expression** for the disordered divergence

$$p_{DO}\left(\kappa = \frac{1}{2} - \alpha\right) = \frac{4}{\pi E_G}\int_{1-\sqrt{E_G}}^{1}\int_{1-\sqrt{E_G}}^{1}\frac{\Theta(xy-2\kappa)}{\sqrt{x^2y^2-4\kappa^2}}dxdy$$

$$\begin{aligned} = \quad & S_{DO}(\kappa,1,1) - S_{DO}(\kappa,1,1-\sqrt{E_G}) \\ & -S_{DO}(\kappa,1-\sqrt{E_G},1) + S_{DO}(\kappa,1-\sqrt{E_G},1-\sqrt{E_G}). \end{aligned} \tag{22}$$

- with

$$S_{DO}(\kappa,x,y) = \int\int \frac{1}{\sqrt{x^2y^2-4\kappa^2}}dxdy$$

$$\begin{aligned} = \quad & -\frac{1}{2}\mathrm{Li}_2\left(\frac{2\kappa^2}{2\kappa^2 - xy\left(xy+\sqrt{x^2y^2-4\kappa^2}\right)}\right) - \frac{1}{2}\log^2\left(\sqrt{x^2y^2-4\kappa^2}+xy\right) \\ + \quad & \log(xy)\log\left(\sqrt{x^2y^2-4\kappa^2}+xy\right) \\ + \quad & \log(2)\log\left(\frac{\sqrt{x^2y^2-4\kappa^2}}{x}+y\right) + \frac{1}{2}\log(\kappa)\log\left(\frac{\kappa}{x^2}\right) + \frac{1}{2}\log^2(y) - \frac{\pi^2}{8} - \frac{1}{2}\log^2(2), \end{aligned} \tag{23}$$

Comparision with Simulations

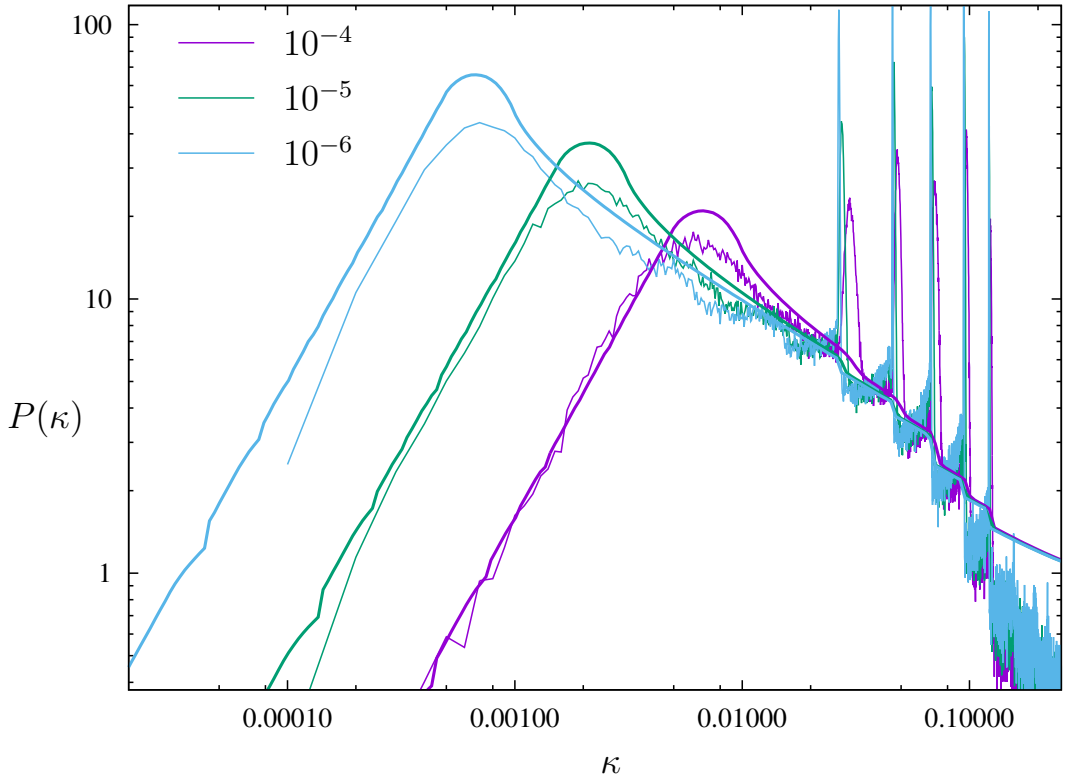

Figure: Comparision between the distributions of $\kappa = \frac{1}{2} - \alpha$ obtained from the theory and numerical simulations at three different energies. The theoretically obtained distributions are plotted with bold lines.

Scaling Form

- The disordered divergence has the following **scaling form**

$$p_{DO}(\alpha) = {E_G}^{-1/4} \mathcal{P}_{DO}\left(\frac{\frac{1}{2} - \alpha}{\sqrt{E_G}}\right). \tag{24}$$

- which possesses the following **asymptotic behaviour**

$$\mathcal{P}_{DO}(x) \sim \begin{cases} x^{3/2}\ , \ x \to 0, \\ \\ x^{-1/2}\ , \ x \to \infty\ . \end{cases} \tag{25}$$

- Similarly we find that the "ordered" distribution has a scaling form

$$p(\alpha, 3) = {E_G}^{-1/2} \mathcal{P}_O\left(\frac{\frac{\sqrt{3}}{4} - \alpha}{\sqrt{E_G}}\right), \tag{26}$$

- which is **integrable in the** $E_G \to 0^+$ **limit**.

Global Scaling

- The **overall density of states** is given by

$$g(\alpha) = N_C \left(p(\alpha, 3) + p(\alpha, > 3) \right), \tag{27}$$

with

$$p(\alpha, > 3) = p_{\text{reg}}(\alpha) + \underbrace{p_{DO}(\alpha)}_{\Delta E^{-1/4}}. \tag{28}$$

- The **regularity of** $g(\alpha)$ **at** $E_G = 0$ leads to

$$N_C = \frac{\int_0^{1/2} g_{\text{reg}}(\alpha) d\alpha}{p(\alpha, > 3) - \Delta}. \tag{29}$$

- Which implies the **scaling of the excess coordination**

$$\Delta Z \sim E^{1/4}. \tag{30}$$

Conclusions

- We developed a **statistical framework for the unjamming transition** of soft frictionless disks in two dimensions.
- We used **local grain areas assigned to each contact** as the microscopic degrees of freedom with which to describe the system.
- We found that large scale **numerical simulations match the predictions** very well.
- For Hertzian potentials with exponent β, the scaling with energy is replaced with exponent $1/2\beta$, however the **underlying scaling forms remain unchanged**.
- It would be interesting to extend this analysis to systems with **different shapes of particles** and **frictional systems**.

Acknowledgements

C. S. O'Hern, T. Bertrand, Q. Wu, D. Dhar, A. Narayanan

Thank You.